



Interrogation of gossypol therapy in glioblastoma implementing cell line and patient-derived tumour models

The Harvard community has made this article openly available. [Please share](#) how this access benefits you. Your story matters

Citation	Jarzabek, M. A., V. Amberger-Murphy, J. J. Callanan, C. Gao, A. M. Zagodzón, L. Shiels, J. Wang, et al. 2014. "Interrogation of gossypol therapy in glioblastoma implementing cell line and patient-derived tumour models." <i>British Journal of Cancer</i> 111 (12): 2275-2286. doi:10.1038/bjc.2014.529. http://dx.doi.org/10.1038/bjc.2014.529 .
Published Version	doi:10.1038/bjc.2014.529
Citable link	http://nrs.harvard.edu/urn-3:HUL.InstRepos:23993536
Terms of Use	This article was downloaded from Harvard University's DASH repository, and is made available under the terms and conditions applicable to Other Posted Material, as set forth at http://nrs.harvard.edu/urn-3:HUL.InstRepos:dash.current.terms-of-use#LAA

Keywords: GBM; gossypol; TMZ; angiogenesis; apoptosis; invasion

Interrogation of gossypol therapy in glioblastoma implementing cell line and patient-derived tumour models

M A Jarzabek¹, V Amberger-Murphy^{2,3}, J J Callanan^{4,5}, C Gao⁶, A M Zagozdzon⁷, L Shiels¹, J Wang⁸, K L Ligon⁹, B E Rich⁹, P Dicker¹⁰, W M Gallagher⁷, J H M Prehn¹ and A T Byrne^{*,1,7}

¹Department of Physiology and Medical Physics and Centre for Systems Medicine, Royal College of Surgeons in Ireland, Dublin 2, Ireland; ²Molecular Therapeutics for Cancer Ireland, Dublin City University, Dublin 9, Ireland; ³All Ireland Cooperative Oncology Research Group, Dublin 2, Ireland; ⁴UCD School of Veterinary Medicine, University College Dublin, Dublin 4, Ireland; ⁵Ross School of Veterinary Medicine, Basseterre, St Kitts, West Indies; ⁶Department of Biological Engineering, Massachusetts Institute of Technology, Cambridge, MA, USA; ⁷UCD School of Biomolecular and Biomedical Science, UCD Conway Institute, University College Dublin, Dublin 4, Ireland; ⁸Department of Biomedicine, University of Bergen, Bergen, Norway; ⁹Department of Medical Oncology, Dana-Farber Cancer Institute, Harvard Medical School, Boston, MA, USA and ¹⁰PHS Department of Epidemiology and Public Health Medicine, Royal College of Surgeons in Ireland, Dublin 2, Ireland

Background: Glioblastoma (GBM), being a highly vascularised and locally invasive tumour, is an attractive target for anti-angiogenic and anti-invasive therapies. The GBM/endothelial cell response to gossypol/temozolomide (TMZ) treatment was investigated with a particular aim to assess treatment effects on cancer hallmarks.

Methods: Cell viability, endothelial tube formation and GBM tumour cell invasion were variously assessed following combined treatment *in vitro*. The U87MG-luc2 subcutaneous xenograft model was used to investigate therapeutic response *in vivo*. Viable tumour response to treatment was interrogated using immunohistochemistry. Combined treatment protocols were also tested in primary GBM patient-derived cultures.

Results: An endothelial/GBM cell viability inhibitory effect, as well as an anti-angiogenic and anti-invasive response, to combined treatment have been demonstrated *in vitro*. A significantly greater anti-proliferative ($P=0.020$, $P=0.030$), anti-angiogenic ($P=0.040$, $P<0.0001$) and pro-apoptotic ($P=0.0083$, $P=0.0149$) response was observed when combined treatment was compared with single gossypol/TMZ treatment response, respectively. GBM cell line and patient-specific response to gossypol/TMZ treatment was observed.

Conclusions: Our results indicate that response to a combined gossypol/TMZ treatment is related to inhibition of tumour-associated angiogenesis, invasion and proliferation and warrants further investigation as a novel targeted GBM treatment strategy.

Glioblastoma (GBM) represents the most common and aggressive form of malignant brain tumour and is classified as a grade IV glioma by the World Health Organization. It is characterised by the presence of multifocal necrosis, microvascular proliferation, local tumour cell invasion and inherent resistance to apoptosis (Louis

et al, 2007). Despite current standard of care, which includes surgery, radiation and chemotherapy with the alkylating agent temozolomide (TMZ), survival rates for GBM remains low. Median survival for patients is just 14 months from the time of diagnosis (Stupp *et al*, 2005, 2009).

*Correspondence: Dr AT Byrne; E-mail: annettebyrne@rcsi.ie

Received 4 July 2014; revised 7 September 2014; accepted 8 September 2014; published online 6 November 2014

© 2014 Cancer Research UK. All rights reserved 0007–0920/14

Angiogenesis has a crucial role in GBM tumour growth, maintenance and local spread throughout the brain. The formation of abnormal vasculature and local tumour cell invasion often results in resistance to conventional treatment (Onishi *et al*, 2011). Therefore, as we have previously suggested (Jarzabek *et al*, 2013b), the development of novel therapeutics, which inhibit more than one 'hallmark of cancer' (e.g., angiogenesis, GBM cell invasion, proliferation and/or apoptosis) and which act synergistically with standard treatment regimens, remains a critical objective.

One promising approach may be inhibition of pro-survival B-cell lymphoma (Bcl-2) proteins (Azmi and Mohammad, 2009). It has been demonstrated that Bcl-2 proteins enhance tumour progression (through inhibition of apoptosis) (Adams and Cory, 2007; Chipuk *et al*, 2010), neo-angiogenesis (through induction of the hypoxia-inducible factor-1 transcription factor, endothelial cell survival and VEGF) (Biroccio *et al*, 2000; Fernandez *et al*, 2001; Kumar *et al*, 2008), tumour invasion (through induction of matrix metalloproteinases (MMPs)) (Wick *et al*, 1998; Choi *et al*, 2005) and resistance to chemotherapeutic agents, such as TMZ (Krakstad and Chekenya, 2010). Moreover, upregulated Bcl-2 expression has been shown in microvascular endothelial cells resulting in increased tumour angiogenesis and tumour growth (Nor *et al*, 2001).

Gossypol, a small molecule, naturally occurring BH3 mimetic, is a cottonseed-derived polyphenolic compound that has been extensively tested in humans as a male contraceptive agent (Qian and Wang, 1984), where it was shown to preferentially inhibit cellular energy metabolism by inhibiting redox reactions catalysed by lactate dehydrogenase A (LDH-A) (Javed and Khan, 1999; Connors *et al*, 2005). Gossypol binds to the BH3 groove of Bcl-2 ($K_i = 320$ nM), Bcl-X_L ($K_i = 480$ nM) and Mcl-1 ($K_i = 180$ nM) (Qiu *et al*, 2002) and decreases the proliferation of many human cancer cells both in *in vitro* and *in vivo* settings (Mohammad *et al*, 2005; Wolter *et al*, 2006; Meng *et al*, 2008; Pang *et al*, 2011), including GBM (Coyle *et al*, 1994; Voss *et al*, 2010). Recent studies suggest a direct role for the drug in suppression of angiogenesis (Pang *et al*, 2011) and metastatic behaviour (Huang *et al*, 2009; Jiang *et al*, 2011).

Gossypol has also been tested in patients with recurrent or progressive GBM in early clinical trials. It has been shown to be well tolerated at a dose of 20 mg day⁻¹ and has a low, but measurable, response rate (Bushunow *et al*, 1999). In addition, two clinical trials with gossypol have been completed: (i) a phase II trial to determine the acute and late toxicity of single-agent gossypol treatment with patients having progressive or recurrent GBM (NCT00540722) and (ii) a non-randomised phase I trial to investigate the side effects and dosage of gossypol in combination with TMZ with or without radiation therapy with patients having newly diagnosed GBM (NCT00390403). Results from these clinical studies are not yet available.

In the present study, the response to targeting multiple 'hallmarks of cancer' with gossypol, alone and in combination with TMZ, in GBM was investigated, implementing *in vitro* and *in vivo* disease models. Synergy and/or additive effects of the combined treatment were assessed *in vitro*, as well as the pro-apoptotic, anti-proliferative, anti-angiogenic and anti-tumour invasive response.

MATERIALS AND METHODS

Reagents. Gossypol and TMZ were purchased from Sigma-Aldrich, St. Louis, MO, USA. For *in vitro* experiments, reagents were dissolved in DMSO at 100 mM stock solution. For *in vivo* studies, gossypol was solubilised in a vehicle solution of 10% ethanol in sterile dH₂O (Xu *et al*, 2005), whereas TMZ was

formulated in a vehicle solution of 10% DMSO in sterile D-PBS (Pedretti *et al*, 2010) as previously described. Both agents were freshly prepared before each administration.

Cell cultures. U87MG-luc2 GBM cell line was purchased from Caliper Life Science (A PerkinElmer Company, Hopkinton, MA, USA) and cultured in Eagle's Minimum Essential Medium (EMEM) (Gibco, Invitrogen, Carlsbad, CA, USA). U251, U373 and U343 GBM cell lines were purchased from the American Tissue Culture Collection (ATCC, Rockville, MD, USA) and cultured in high-glucose (4500 mg l⁻¹) Dulbecco's Modified Eagle's Medium (DMEM) (Lonza, Basel, Switzerland). EMEM and DMEM were supplemented with 10% heat-inactivated foetal bovine serum (FBS), 1% L-glutamine (2 mM) and 1% penicillin/streptomycin (50 units ml⁻¹), all from Sigma-Aldrich. Human umbilical vein endothelial cells (HUVECs) were purchased from Lonza and maintained in Endothelial Cell Basal Medium-2 (EBM-2, Lonza). Each 500 ml of EBM-2 was supplemented with EGM-2 SingleQuots Kit (Lonza) consisting the following growth supplements: human epidermal growth factor (hEGF), 0.5 ml; vascular endothelial growth factor (VEGF), 0.5 ml; R3-insulin-like growth factor-1 (R3-IGF-1), 0.5 ml; ascorbic acid, 0.5 ml; hydrocortisone, 0.2 ml; human fibroblast growth factor-beta (hFGF-β), 2.0 ml; heparin (0.5 ml); fetal bovine serum (FBS), 25.0 ml; gentamicin/amphotericin-B (GA), 0.5 ml. All cells were maintained at 37 °C in humidified air with 5% CO₂.

3-(4, 5-Dimethylthiazol-2-yl)-2, 5-diphenyltetrazolium bromide, a yellow tetrazole (MTT)-based cell viability assay. Cell viability was determined using the MTT reagent (Sigma-Aldrich). GBM cell lines or HUVECs were seeded into 96-well cell culture plates (2000 GBM cells 100 μl⁻¹ well⁻¹ or 5000 HUVECs 100 μl⁻¹ well⁻¹). Following incubation (24 h), 100 μl of medium with or without test agent(s) was added into appropriate wells and incubated for the desired periods. Following incubation, 20 μl of MTT in D-PBS (5 mg ml⁻¹) was added to each well. After 4 h, medium was replaced with 100 μl of DMSO in order to dissolve MTT formazan product. Absorbance was read on a spectrophotometer at 560 nm. Drug concentrations causing 50% cell growth inhibition (IC₅₀ values) were calculated for single drug treatment via a sigmoidal dose-response curve using GraphPad Prism version 5.00 for Windows (Graphpad, San Diego, CA, USA). The dose-effect analysis by Chou and Talalay (1984) was used to assess the interaction between gossypol and TMZ. Determination of the synergistic, additive and/or antagonistic cytotoxic effects of the combined treatment of GBM cells and HUVECs was assessed using the CompuSyn for Drug Combinatios and for General Dose-Effect Analysis software (ComboSyn, Inc., Paramus, NJ, USA). The combination index (CI) was used to express synergism (CI < 1), additive effect (CI = 1) or antagonism (CI > 1).

***In vitro* endothelial cell capillary-like tube formation assay.** HUVECs were seeded into 96-well cell culture plate coated with matrigel (BD Biosciences, Franklin Lakes, NJ, USA) in the absence/presence of agent(s). Cells were incubated for up to 20 h at 37 °C in CO₂ incubator. Tube formation was observed under a phase-contrast microscope (Nikon, Tokyo, Japan) and a charge-coupled device camera (SPOT RT SE 6; Diagnostic Instruments, Inc., Sterling Heights, MI, USA) at × 200 magnification. Four randomly chosen microscopic fields per well were photographed with a digital camera. The number of branch-points per field-of-view was counted, and the length of tubules was quantified using the ImageJ 1.44 software (NIH, Bethesda, MD, USA).

3-D invasion assay. GBM cell line spheroids were formed using the hanging drop method previously described (Del Duca *et al*, 2004). Following incubation (48 h), cell aggregates were transferred to a 100-mm dish coated with 2% agar filled with 10 ml of growth medium. Following incubation (48 h), spheroids were implanted

into collagen gel (one spheroid per well and 500 μl of collagen solution per well in 24-well plate). Chilled *PureCol* Bovine Collagen Product 3 mg ml⁻¹ (Nutacon BV, Leimuiden, The Netherlands) was mixed with 10-fold concentrated Dulbecco's minimal essential medium (Sigma-Aldrich) and cold 0.1 M sodium hydroxide (Sigma-Aldrich) at a ratio of 8 : 1 : 1. pH was neutralised by adding 1 M NaOH (Sigma-Aldrich). Following incubation in 37 °C (1 h), 500 μl of complete growth medium was added to each well and returned to incubator. Gossypol (either with or without TMZ) was re-suspended in growth medium and added to the collagen gel matrix 2 days after implantation of spheroids into collagen gel (when invasion had already started). Cell invasion out of the spheroid was measured before treatment commenced (day 0) and on days: 2, 6, 8, 13 and 15, using a grating objective, a phase-contrast microscope (Nikon). Images were taken with a charge-coupled device camera (SPOT RT SE 6; Diagnostic Instruments, Inc.) at day 15. Alternatively, a 3-D matrigel invasion assay was performed as previously described (Kwiatkowska *et al*, 2012) with minor modifications. Briefly, 1×10^5 of U87MG-luc2 cells were re-suspended in 50 μl of BD Matrigel and added to the top well (BD Falcon Cell culture inserts for 24-well plates, 8.0- μm pores, Translucent PET Membrane (BD Biosciences, Franklin Lakes, NJ, USA)). Following incubation at 37 °C for 30 min, 200 μl of serum-free growth medium with or without drug(s) was added to the top well and 700 μl of serum containing growth medium with or without drug(s) to the bottom well. After 48 h, cells attached to the bottom of insert were fixed and stained with 0.5% methylene blue dissolved in dH₂O (Sigma-Aldrich). Cells on the upper surface of the filter were wiped off with a Q-tip. Images were taken using a colour device camera.

GBM xenograft model and drug treatment. All animal experiments were licensed by the Department of Health and Children in Ireland. Study protocols were reviewed by the Animal Research Ethics Committee (AREC) at the University College Dublin. Female BALB C nu/nu mice (4–6 weeks) were procured at the SPF-grade Conway Institute Biotechnical Services (CIBS) Xenograft Facility from Harlan Laboratories, UK, Ltd., Bicester, UK. Mice were anaesthetised with O₂/isoflurane mixture, and 5×10^6 of U87MG-luc2 cells suspended in 100 μl of matrigel/D-PBS mixture (50 : 50) were inoculated subcutaneously in the right flank of the animal. Tumour dimensions were measured by calliper, and volumes estimated by the formula: $a^2 \times b \times 0.5$, where a and b are the shorter and longer diameter of the tumours, respectively. When tumours reached approximately 200 mm³ (approximately 28 days following inoculation), mice were randomised into treatment groups. No difference in mean tumour volume was observed among the treatment groups at day 0 before treatment commencement. Group 1 ($n=8$) received 30 mg kg⁻¹ of gossypol by oral gavage (p.o.), using a regiment of daily dosing for 5 consecutive days, followed by a 2-day rest, before resuming dosing. Group 2 ($n=6$) was treated with 7.5 mg kg⁻¹ of TMZ by intraperitoneal injection (i.p.) daily for 9 consecutive days. Group 3 ($n=8$) received both gossypol and TMZ treatments using the same regimens as above. On days when both drugs were administered, TMZ was administered at least 5 h after gossypol. The control cohort received an equivalent volume of vehicle for gossypol (10% ethanol in sterile dH₂O) and TMZ (10% DMSO in sterile D-PBS). All animals were monitored for adverse effects. When tumours exceeded 15 mm in any of the diameters, animals were euthanised.

Histological examination and immunohistochemistry. Subcutaneous tumours were excised, rinsed twice in D-PBS and fixed in 4% formaldehyde for 48 h. Tissues were embedded in paraffin and 5- μm thick sections were cut. Sections were deparaffinised with histoclear II and re-hydrated according to standard histological procedures. Routine hematoxylin and eosin (H&E) staining was performed to facilitate histological evaluation by a veterinary

pathologist. For immunohistochemistry, epitope retrieval was performed by microwave boiling for 20 min in 10 mM citrate buffer at pH 6.0. One hour blocking in 5% serum/TBS-T was used before primary antibody incubation (rabbit anti-human Ki67 (Millipore, Billerica, MA, USA, dilution 1 : 100) for 1 h in room temperature or goat anti-PECAM-1/Cd31 (Santa Cruz Biotechnology, Santa Cruz, CA, USA, dilution 1 : 100) overnight at 4 °C). Biotinylated goat anti-rabbit or horse anti-goat secondary antibody, respectively (Vector Laboratories, Burlingame, CA, USA, dilution 1 : 200), were applied for 1 h at room temperature followed by ABC-complex (Vectastain ABC kit, Vector Laboratories) incubation for 30 min. Signal was developed with diaminobenzidine (DAKO Cytomation, Glostrup, Denmark) according to the manufacturer's instructions. Sections were counterstained with hematoxylin (Sigma-Aldrich) to visualise nuclei. For assessment of proliferation indices, percentage of Ki-67-positive cells in the viable areas of tumours was quantified under a light microscope, using an objective with grid-graticula. Microvessel density was assessed using an anti-PECAM-1/CD31 antibody. Vessel counts were performed as previously described (Leonard *et al*, 2008).

TUNEL staining. The ApopTag Peroxidase In Situ Apoptosis Detection Kit (Millipore) was used to detect apoptotic cells *in situ* according to the manufacturer's protocol.

Human GBM tumour-derived multicellular spheroid culture. Human GBM tumour-derived spheroids (patient 3) were kindly provided by Professor Rolf Bjerkvig (University of Bergen) and expanded *in vivo* via serial transplantation into immunocompromised rodents as previously described (Bjerkvig *et al*, 1990; Wang *et al*, 2009; Johannessen *et al*, 2009). Human GBM tumour-derived multicellular spheroids were maintained for short term *in vitro* in complete growth medium (DMEM (Sigma-Aldrich), containing 10% FBS supplemented with nonessential amino acids, 100 U ml⁻¹ penicillin/streptomycin and 400 mM L-glutamine (all from Cambrex, East Rutherford, NJ, USA) as previously described (Jarzabek *et al*, 2013a).

Human GBM tumour-derived neurosphere lines culture. GBM neurosphere lines (BT224-luc2 and BT248-luc2) were derived from Brigham and Women's Hospital patients undergoing surgery according to IRB-approved protocols as previously described (Mehta *et al*, 2011; Koivunen *et al*, 2012). Briefly, GBM tumour resection samples were mechanically dissociated, and neurospheres were established and propagated in Complete Human NeuroCult NS-A Proliferation Medium that contains NeuroCult NS-A Basal Medium, NeuroCult NS-A Proliferation Supplements, 20 ng ml⁻¹ rh-EGF, 10 ng ml⁻¹ rh-bFGF and 2 μg ml⁻¹ heparin (StemCell Technologies, Vancouver, BC, Canada) as previously described (Inda *et al*, 2010). Cells were maintained and expanded in ultra-low-attachment 25-cm² cell culture vessels. Luciferase expression of human GBM tumour-derived neurosphere lines was performed as previously described using pMMP-LucNeo retrovirus (Rubin *et al*, 2003). Human GBM tumour-derived BT-224-luc2 and BT248-luc2 neurosphere lines used in this study were passaged not more than 10 times.

Human GBM tumour-derived spheroids and neurosphere lines *in vitro* viability assays. Human GBM tumour-derived spheroids were transferred to 96-well plate (one spheroid per well) and cultured in complete growth medium as previously described (Johannessen *et al*, 2009). Whereas, GBM patient-derived neurospheres were mechanically dissociated and re-suspended in complete NeuroCult medium and seeded 2000 cells per 100 μl of complete NeuroCult medium per well as previously described (Ziegler *et al*, 2011). Following overnight culture, 100 μl of complete growth medium containing DMSO (control wells) or drug(s) in appropriate concentration (treated wells) were added. Following incubation (37 °C in humidified air with 5% CO₂ for

96 h), 20 μl of MTT/PBS (5 mg ml^{-1}) was added into each well. Following incubation (4 h), plates were spun down at 2000 r.p.m. for 5 min. Subsequently, media containing MTT solution was carefully removed from each well, and crystals were dissolved in 100 μl of DMSO. Well content was agitated for 15 min on a micro-plate shaker. Finally, absorbance at 560 nm of the resulting solution was measured using a micro-plate reader (Tecan Group Ltd, Männedorf, Switzerland).

Statistical methods. For statistical comparison, a mixed-model linear test analysis (SPSS, IBM Corporation, Armonk, NY, USA), unpaired *t*-test or one-way analysis of variance (ANOVA) followed by Tukey's *post-hoc* test (GraphPad Prism version 5.00 for Windows, San Diego, CA, USA) was employed.

RESULTS

Gossypol acts synergistically with TMZ to inhibit endothelial cells (HUVECs) and GBM (U87-MG-luc2 and U343) cell lines. To investigate the dose-dependent cytotoxic effect of gossypol on GBM and endothelial cells and to estimate and compare IC_{50} concentrations, four GBM cell lines (U87MG-luc2, U251, U373, U343) (Figure 1A) and HUVECs (Figure 1B) were treated with different concentrations of gossypol for 72 h. Mean IC_{50} values, for each GBM cell line and endothelial cells, were obtained. Enhanced gossypol cytotoxicity was observed in HUVECs showing lowest IC_{50} concentration (1.699 \pm 0.178) when compared with IC_{50} concentrations derived for four different GBM cell lines. Among the GBM cell lines tested, U251 and U373 exhibited higher IC_{50} values following 72 h treatment (11.600 \pm 4.353 and 10.120 \pm 2.931, respectively) when compared with U343 and U87 cell lines (5.784 \pm 0.458 and 5.689 \pm 0.487, respectively) (Figure 1C).

To examine the sensitivity of GBM cells to combined gossypol/TMZ treatment, U87MG-luc2, U251, U373 and U343 cells were exposed to various concentrations of gossypol (3, 6 or 12 μM) either with or without differing concentrations of TMZ (100, 200 or 400 μM) for 96 h (Figure 2). Maximum growth inhibition (400 μM TMZ) did not exceed 52, 53, 27 or 52% in U87MG-luc2, U251, U343 or U373 cell lines, respectively. Addition of gossypol enhanced the anti-proliferative effect of TMZ, increasing growth inhibition to 89, 70, 63 or 82%, respectively, in U87MG-luc2, U251, U343 or U373 cell lines (one-way ANOVA, $P < 0.05$). Combining TMZ with gossypol (3 μM) potentiated the effect of gossypol alone (Figure 2A, C, E and G). Isobologram analysis was employed to further investigate whether observed gossypol and TMZ interactions were antagonistic, additive or synergistic. CI values $<$, $=$ or $>$ 1 indicate synergy, additive effect or antagonism, respectively. The greatest synergistic interaction was observed in the U343 cell line, some synergistic interaction was observed in U87MG-luc2 cell line, whereas U251 and U373 cell lines exhibited additive and antagonistic responses to gossypol/TMZ treatment (Figure 2B, D, F, H and K).

Next, sensitivity of HUVECs to combined gossypol/TMZ treatment was examined. HUVECs were exposed to various concentrations of gossypol (1.5, 3 or 6 μM) either with or without various concentrations of TMZ (50, 100 or 200 μM) for 72 h. As HUVECs are more sensitive to gossypol treatment, lower drug concentrations and shorter incubation times were used to assess treatment efficacy. Maximum growth inhibition with 200 μM of TMZ did not exceed 30%. Nevertheless, the addition of gossypol greatly enhanced the anti-proliferative effect of TMZ, causing up to 88% growth inhibition in HUVECs. Combining TMZ with 1.5 μM gossypol appeared to potentiate the effect of single-agent gossypol (Figure 2I). Similarly, in order to further analyse drug combination response in HUVECs, isobologram analysis was performed.

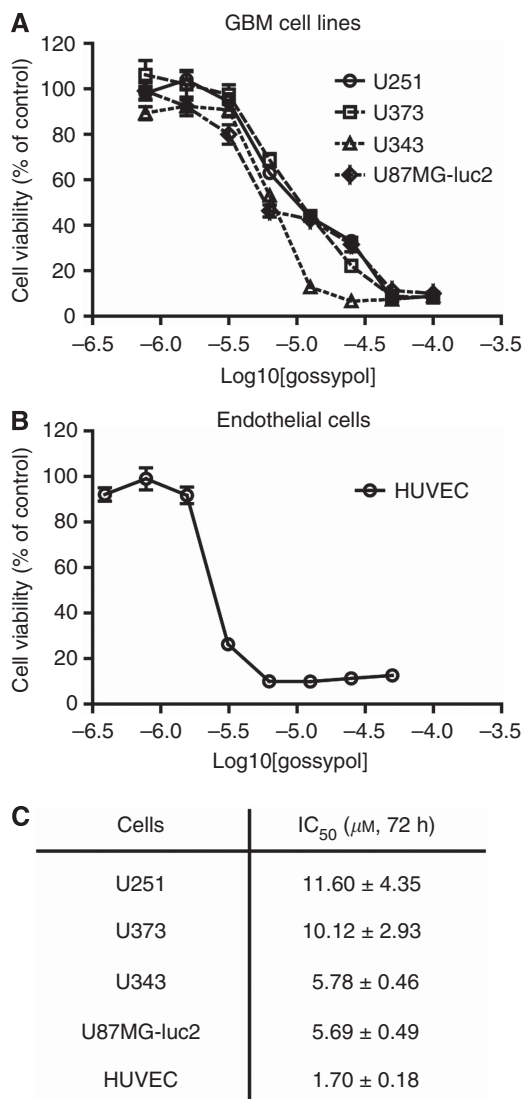


Figure 1. Gossypol reduces endothelial and GBM cell viability in a dose-dependent manner. (A) The human GBM cell lines (U251, U373, U343, U87MG-luc2) and (B) HUVECs were exposed to various concentrations of gossypol for 72 h. GBM/endothelial cell viability was assessed using the MTT-based cell viability assay. Each treatment condition was replicated in at least three wells and in three independent experiments. (C) IC_{50} concentrations were estimated based on sigmoidal dose-response curves using the GraphPad software. Mean \pm s.e.m. of three independent experiments are presented.

Analysis of CIs provided evidence that the majority of treatment conditions implemented in HUVEC studies promoted synergistic cell killing (Figure 2J and K).

Gossypol in combination with TMZ treatment inhibits HUVEC tube formation *in vitro*. In order to further examine the effects of gossypol/TMZ treatment on the final step of angiogenesis, (tubulogenesis), we employed an *in vitro* tubule-formation assay (Figure 3A–H). Tubule length (Figure 3I) and branch point (Figure 3J) analyses demonstrated significant inhibition of both tubule length and branch points in a dose-dependent manner following 20-h gossypol/TMZ treatment ($P < 0.05$ when compared with control). Moreover, comparison of combined gossypol/TMZ treatment with single-agent TMZ treatment revealed a significant decrease in the total tubule length (when gossypol was used at 3, 6

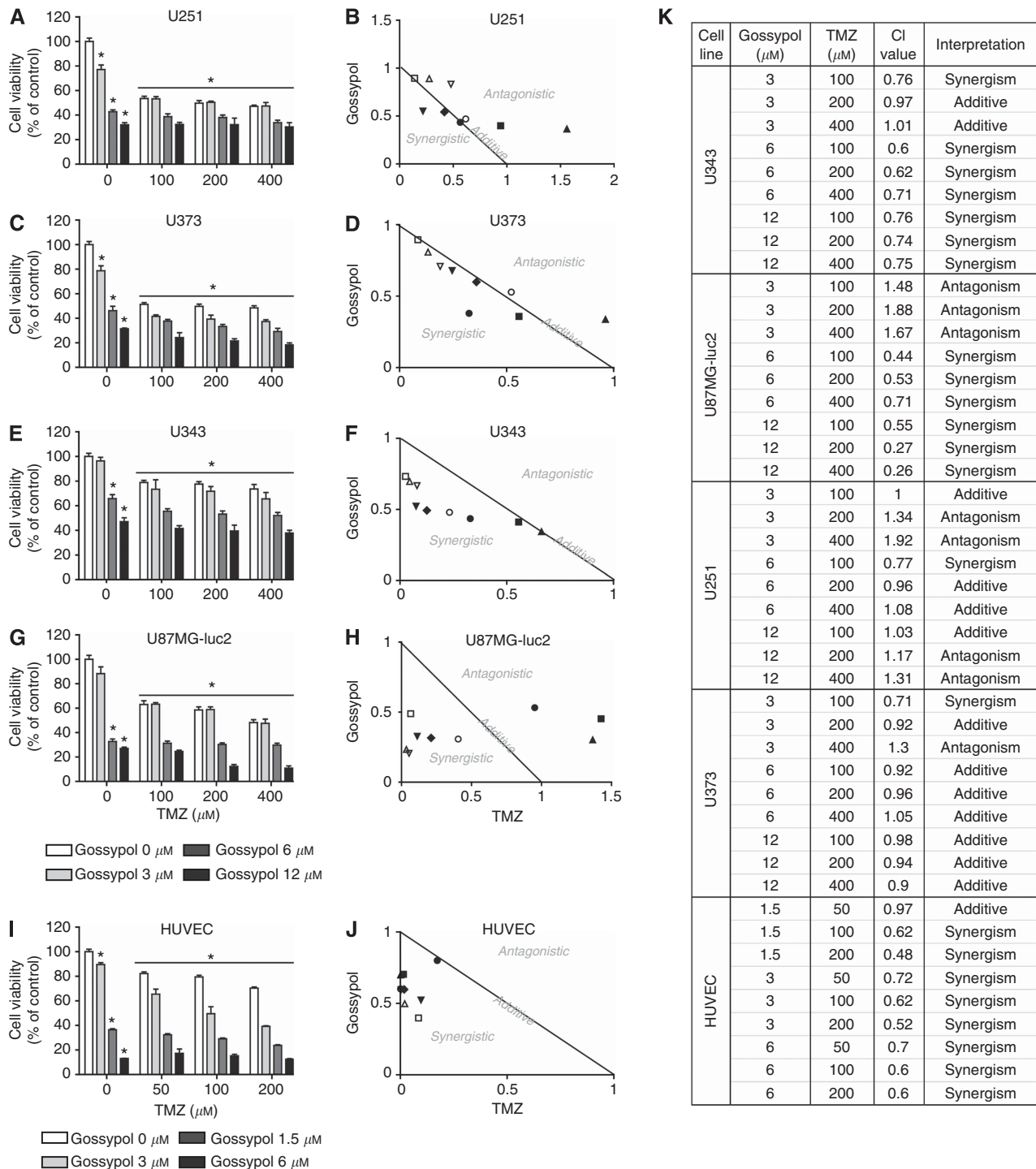


Figure 2. Synergistic response to gossypol and TMZ combination therapy in GBM cell lines and primary endothelial cultures. (A–H) GBM and (I, J) endothelial cells were exposed to increasing concentrations of gossypol and/or TMZ for 96 or 72 h, respectively. Cell viability was assessed using the MTT assay. Each treatment condition was replicated in at least three wells and in three independent experiments. Means \pm s.e.m. of three independent experiments are presented. * $P < 0.05$ compared with control (0 μM gossypol + 0 μM TMZ), one-way ANOVA and Tukey's *post-hoc* test (A, C, E, G, I). The combination indices (CIs) corresponding to the gossypol/TMZ combinations tested in figures (A, C, E, G, I) were determined by the CompuSyn software (B, D, F, H, J, K). A normalised isobolograms (B, D, F, H, J) graphically represent the interaction between gossypol and TMZ, whereas (K) summary table lists all the CI values obtained from the analysis and their interpretations. The combination index (CI) was used to express synergism (CI < 1), additive effect (CI = 1) or antagonism (CI > 1).

or 12 μM concentrations) and number of branch points (when gossypol was used at 6 or 12 μM concentrations). Comparison of combined gossypol/TMZ treatment with single gossypol treatment showed a significant decrease in the total tubule length and number of branch points when gossypol was implemented at concentrations of 3 and 6 μM (Figure 3I and J).

Gossypol in combination with TMZ treatment inhibits GBM cell invasion *in vitro*. To investigate GBM cell invasion following gossypol \pm TMZ treatment *in vitro*, we first employed a 3-D spheroid invasion assay using the U87MG-luc2 GBM cell line. In a control setting, U87MG-luc2 GBM cells demonstrated invasive activity reaching a distance of $3746.528 \pm 127.625 \mu\text{m}$ from parent

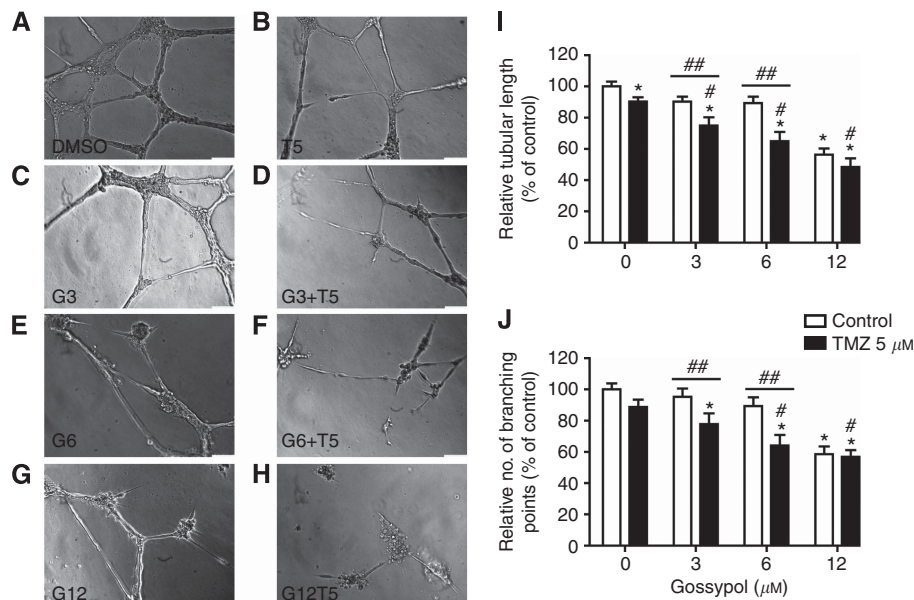


Figure 3. Gossypol in combination with TMZ inhibits endothelial cell tube formation *in vitro*. HUVECs were seeded on BD Matrigel in the presence or absence of gossypol (3, 6 or 12 μM) with or without TMZ (5 μM) and incubated for 20 h. Representative images of (A) control, (B) gossypol (3 μM)-, (C) gossypol (6 μM)-, (D) gossypol (12 μM)-, (E) TMZ (5 μM)-, (F) gossypol (3 μM)/TMZ (5 μM)-, (G) gossypol (6 μM)/TMZ (5 μM)- and (H) gossypol (12 μM)/TMZ (5 μM)-treated HUVECs were taken at 20 h time point. Scale bar = 100 μm (\times 200 magnification). (I) Relative tubular length (percentage of control) and (J) relative number of branching points (percentage of control) were quantified. Each treatment condition was replicated in at least three wells and in three independent experiments. Mean \pm s.e.m. are presented. * P <0.05 compared with control, # P <0.05 compared with TMZ treatment, ## P <0.05 compared with gossypol treatment (one-way ANOVA and Tukey's *post-hoc* test).

spheroid within 15 days. U87MG-luc2 cells treated with gossypol (3, 6 or 12 μM)/TMZ (100 μM) combination invaded to a lesser extent from the spheroid core through the collagen gel (Figure 4A–H). Significant anti-invasive effects of U87MG-luc2 cells treated with the combination regimen were observed in comparison to the invasion distance in control wells commencing from day 6 when 3 μM of gossypol was used and from day 4 when higher concentration (6 or 12 μM) of gossypol was used in combination with TMZ (100 μM) treatment. Moreover, spheroids treated with combined gossypol/TMZ treatment showed a significant difference when compared with single treatments as indicated in Figure 4I–K. Quantification of average invasion distance per day revealed that spheroids treated with the combination regimen gossypol (6 or 12 μM)/TMZ (100 μM) invaded at a significantly slower rate when compared with control (Figure 4L). The *in vitro* effect of gossypol treatment delivered in combination with TMZ on GBM cell invasion was further confirmed in 3-D matrigel invasion assay using trans-well Boyden chambers as shown in Supplementary Figure S1A–H.

Gossypol in combination with TMZ inhibits GBM cell proliferation, tumour angiogenesis and enhances apoptosis in an *in vivo* GBM setting. To investigate the *in vivo* effect of gossypol either with or without TMZ on tumour growth, proliferation, apoptosis and angiogenesis, we employed a subcutaneous GBM (U87MG-luc2) xenograft mouse model. Tumour growth was measured over time. Figure 5A presents study time points for drug combination treatment, BLI and caliper measurement. Figure 5B shows the mean tumour volume based on caliper measurements over time, and Figure 5C shows bioluminescence images of representative tumours at day 14. As revealed by caliper measurements, tumour volume in the vehicle-treated group indicates rapid and robust tumour growth. An inhibitory effect on tumour growth was observed in animals treated with gossypol \pm TMZ. However, caliper measurements revealed a significant difference in tumour volume only when combined

therapy was compared with single-agent gossypol treatment ($P=0.002$) and not when compared with single-agent TMZ treatment ($P=0.496$) (Figure 5B). Nevertheless, extensive necrotic tumour cores were visible in BLI. Lack of bioluminescence signal or signal reduction in the tumour core indicates haemorrhagic and necrotic areas in rapidly growing tumours (Figure 5C). Differences in the incidence of extensively necrotic tumours between treatment cohorts were observed. Eighty-seven percent of mice displayed an aggressive necrotic phenotype in control cohort, whereas in the single-agent treatment groups (gossypol and TMZ, respectively) this number was reduced to 62% and 50% of mice that had extensive necrotic core. The greatest reduction, only 37% of animals that had necrotic core, was observed in the combination gossypol/TMZ-treated group (Figure 5D).

Further histological analysis of tumour phenotype revealed that control tumours comprised a non-encapsulated densely cellular mass with numerous monomorphic, mononuclear tumour cells similar to the gossypol-treated cohort. Cells were arranged in sheets and clusters in a fine fibrovascular stroma. Necrosis (most likely due to large tumour size/fast growing tumour) was often accompanied by a prominent influx of neutrophils, particularly at the junction of viable and necrotic tissue. In contrast, TMZ monotherapy and combined treatment showed marked distortion of tumour architecture and a prominence of mononuclear giant tumour cells with pleomorphic nuclei and an abundant eosinophilic cytoplasm. Moreover, the pattern of tight clustering of cells in a fibrovascular stroma (seen in vehicle and gossypol cohorts) was frequently lost in regions rich in mononuclear giant cells. Cells in these regions were more loosely arranged and lacking cluster architectures. We observed reduced necrosis in TMZ- and combination-treated tumours. Moreover, control tumours revealed numerous mitotic figure (>5 mitotic figures per high power field (hpf)), whereas tumours treated with either single or combined therapies revealed decreased numbers of mitotic figures (0–3 mitotic figures per hpf) (Figure 5E (H&E images)). A mean count of Ki-67-positive nuclei of 24.86 ± 1.42 was

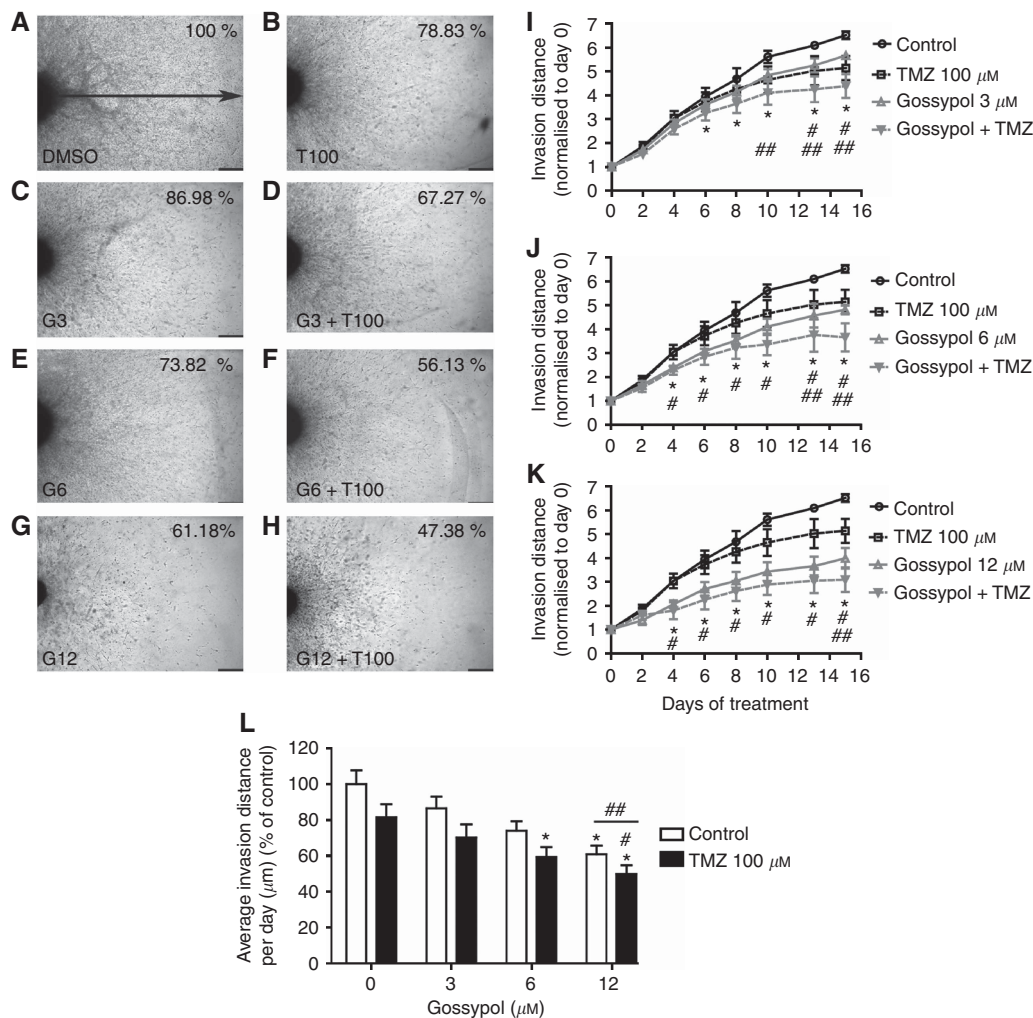


Figure 4. Gossypol in combination with TMZ inhibits GBM cell invasion *in vitro*. U87MG-luc2 spheroids implanted in collagen gel were exposed to gossypol ± TMZ treatment over 15 days. Representative images of (A) control, (B) TMZ (100 μM)-, (C) gossypol (3 μM)-, (D) gossypol (3 μM)/TMZ (100 μM)-, (E) gossypol (100 μM)-, (F) gossypol (6 μM)/TMZ (100 μM)-, (G) gossypol (12 μM)- and (H) gossypol (12 μM)/TMZ (100 μM)-treated spheroids were taken at day 15. Scale bar: 1000 μm (× 40 magnification). Invasion activity of U87MG-luc2 cells exposed to the absence or presence of (I) gossypol (3 μM)/TMZ (100 μM), (J) gossypol (6 μM)/TMZ (100 μM) and (K) gossypol (12 μM)/TMZ (100 μM) over 15 days of treatment, and (L) average invasion distance per day quantified as a percentage of control were quantified. Data presented are mean invasion distance ± s.e.m. of three independent experiments, * $P < 0.05$ compared with the control, # $P < 0.05$ compared with TMZ treatment, ## $P < 0.05$ compared with gossypol treatment, linear mixed model and ANOVA, *post-hoc* Tukey.

observed in vehicle-treated control animals. Single treatments, both gossypol and TMZ, exerted inhibitory effects on actively proliferating GBM cells, showing proliferation index of 15.01 ± 2.12 and 14.71 ± 1.66 , respectively. Statistical analysis indicated that the decrease in proliferation in single gossypol and TMZ-treated animals was significant ($P < 0.0001$ compared with vehicle-treated tumours). Moreover, combined gossypol/TMZ treatment revealed a significantly greater decrease in proliferation compared with single treatments (9.071 ± 0.90 , $P < 0.0001$ compared with vehicle-treated tumours, $P = 0.020$ compared with gossypol-treated tumours, $P = 0.030$ compared with TMZ-treated tumours) (Figure 5E (Ki67 images) and F). The mean percentage of TUNEL-positive cells was 3.958 ± 0.6848 in vehicle-treated control animals. Both single-agent treatments (gossypol and TMZ) exerted pro-apoptotic effects (16.15 ± 3.278 and 16.83 ± 3.715 , respectively). Statistical analysis indicated that the increase in the percentage of TUNEL-positive cells was significant in single-agent-treated cohorts of animals ($P < 0.0001$ compared with vehicle-treated tumours). Moreover, combined gossypol/TMZ treatment revealed a significantly greater increase in the percentage

of TUNEL-positive cells (29.03 ± 3.233 , $P < 0.0001$ compared with vehicle-treated tumours, $P = 0.0083$ compared with gossypol-treated tumours, $P = 0.0149$ compared with TMZ-treated tumours) (Figure 5E (TUNEL images) and G). A mean MVD of 49.63 ± 2.39 was observed in vehicle-treated control animals. Single-agent treatment: gossypol (MVD = 41.70 ± 1.31) and TMZ (MVD = 46.26 ± 2.85) did not show significant inhibitory effects ($P = 0.119$ and $P = 0.731$, respectively, when compared with vehicle cohort). Nevertheless, when combined gossypol/TMZ treatment was used MVD was greatly decreased (MVD = 32.79 ± 2.66) when compared with vehicle ($P < 0.0001$) and single-agent treatment protocols ($P = 0.040$ —combined treatment vs gossypol and $P < 0.0001$ —combined treatment vs TMZ) (Figure 5E (CD31 images) and H).

Gossypol treatment enhances the efficacy of TMZ treatment in GBM patient-derived multicellular spheroids and GBM patient-derived neurosphere cultures. Recent studies have suggested that the response of GBM patient-derived cultures to anti-GBM treatment may better reflect potential therapeutic

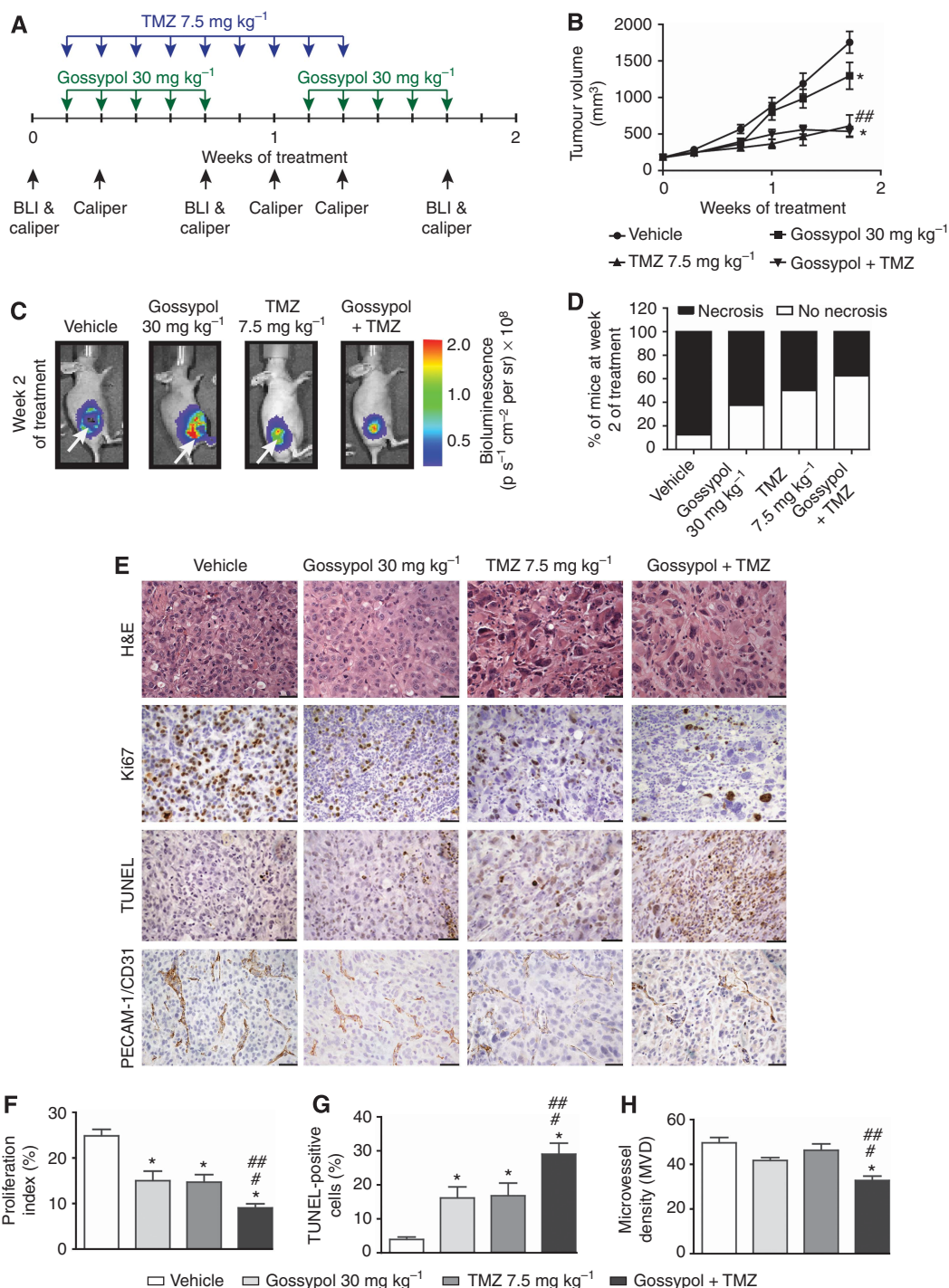


Figure 5. Gossypol in combination with TMZ reduces tumour burden, inhibits angiogenesis and GBM cell proliferation and enhances apoptosis *in vivo*. **(A)** Drug combination treatment, BLI and Caliper measurements time points are presented. **(B)** Tumour volume and **(C)** tumour bioluminescence of each mouse was assessed at different time points. Mean tumour volumes ± s.e.m. (vehicle-treated (n = 6), gossypol 30 mg kg⁻¹-treated (n = 8), TMZ 7.5 mg kg⁻¹-treated (n = 6), combination gossypol/TMZ-treated (n = 8) groups) are shown over time **(B)**. Representative bioluminescent images from second week of treatment are shown for each treatment group **(C)**. **(D)** Incidence of animals (percentage of treatment cohorts) with or without necrotic lesions is shown in bar graph. **(E)** Representative images of H&E, anti-Ki67, TUNEL and anti-PECAM-1/CD31 stained xenograft sections treated with either vehicle, gossypol, TMZ or combination are shown. Scale bars = 50 μm (× 400 magnification, H&E), 100 μm (× 200 magnification, Ki67, TUNEL, PECAM-1/CD31). **(F)** Proliferation index (%), **(G)** TUNEL-positive cells (%) and **(H)** microvessel density (MVD) are shown. Error bars represent mean ± s.e.m. (vehicle-treated (n = 3), gossypol 30 mg kg⁻¹-treated (n = 3), TMZ 7.5 mg kg⁻¹-treated (n = 3), combination gossypol/TMZ-treated (n = 5) tumours); quantifications from five randomly chosen field of views per tumour **(F–H)**. *P < 0.05 compared with vehicle, #P < 0.05 compared with TMZ 7.5 mg/kg, ##P < 0.05 compared with gossypol 30 mg/kg (linear mixed model and ANOVA, post-hoc Tukey).

efficacy *in vitro* than adherent GBM cell lines (Singh *et al*, 2003, 2004; Johannessen *et al*, 2009). We therefore exposed GBM patient-derived cultures to treatment for 96 h. Viability following treatment was assessed using the MTT assay. In contrast to GBM cell lines (U87MG-luc2, U373, U343 and U251), GBM patient-derived multicellular spheroids (Figure 6A) and neurospheres (Figure 6B and C) exhibited greater resistance to TMZ treatment after 96 h. However, a significant reduction in cell viability was observed after single-agent gossypol treatment and combined gossypol/TMZ treatment when compared with control (Figure 6A–C).

DISCUSSION

We have explored the anti-angiogenic, pro-apoptotic, anti-proliferative and anti-invasive properties of treatment with the

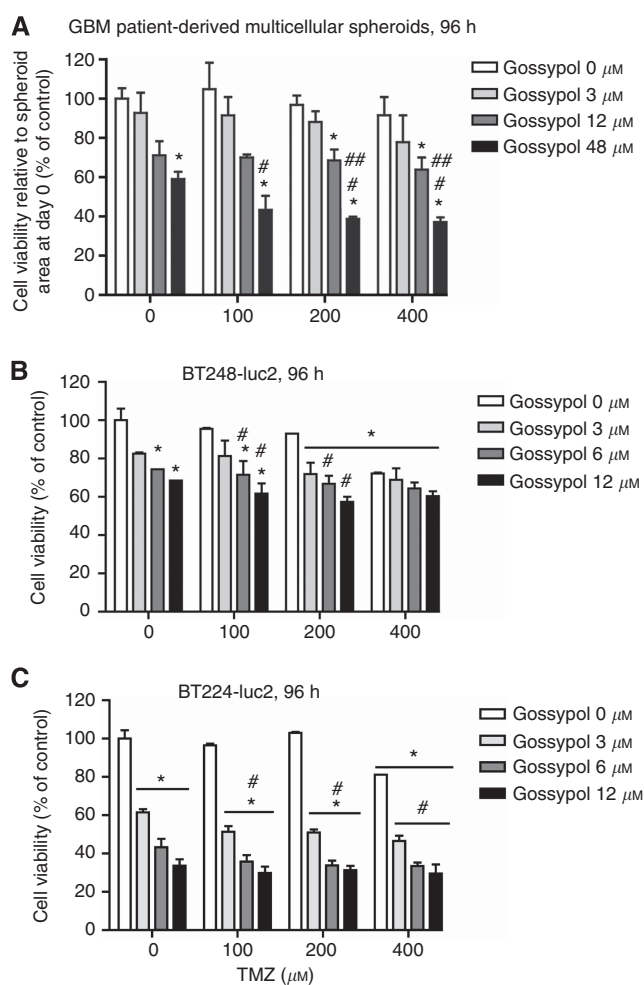


Figure 6. Gossypol in combination with TMZ inhibits human GBM tumour-derived cell viability. Human GBM tumour-derived multicellular spheroids were exposed to gossypol (0, 3, 12, 48 μM) with or without TMZ (0, 100, 200, 400) for 96 h. GBM spheroid viability was assessed using the MTT assay. Each absorbance value was normalised to spheroid area at day 0. (A) At least three spheroids were used per each condition. Human GBM tumour-derived neurosphere cultures (BT248-luc2 and BT224-luc2) were treated for 96 h with gossypol and/or TMZ, and cell viability was assessed using the MTT assay. (B and C) Viability as compared with non-treated controls is shown. Error bars represent mean \pm s.e.m., * $P < 0.05$ compared with the control, # $P < 0.05$ compared with TMZ treatment, ## $P < 0.05$ compared with gossypol treatment, ANOVA and *post-hoc* Tukey.

BH3 mimetic agent gossypol alone and in combination with TMZ, implementing *in vitro* and *in vivo* GBM/endothelial cell models.

In agreement with previous data (Coyle *et al*, 1994; Voss *et al*, 2010; Pang *et al*, 2011), we have shown a dose-dependent cytotoxic effect of gossypol on human GBM and endothelial cells (Figure 1). We tested gossypol alone in four GBM cell lines that differ in Mcl-1 and/or MGMT status (Supplementary Table S1). Our results revealed that U251 and U373 lines were less responsive to gossypol following 72 h treatment than other cell lines tested (U87MG-luc2 and U343). We believe that this may be partially due to Mcl-1 protein levels, which have previously been shown to be lower in U373 and U251 (Day *et al*, 2011). Inhibition of LDH may further contribute (Tuszynski and Cossu, 1984; Coyle *et al*, 1994; Seliger *et al*, 2013). Moreover, we have shown that endothelial cells exhibit greater sensitivity to single-agent gossypol treatment compared with GBM cells. Greater sensitivity of endothelial cells to gossypol was also observed previously when compared with sensitivity of human prostate cancer cells (Pang *et al*, 2011).

It has previously been reported that gossypol potentiates cell death induced by TMZ to a greater extent in cell lines with negative MGMT status (Voss *et al*, 2010). In order to further test this finding, we employed isobologram analysis to investigate the efficacy of combination therapy in four different GBM cell lines of known MGMT status (Figure 2). Greatest synergism between gossypol and TMZ was observed in the U343 line (MGMT-negative) as reported by Voss *et al* (2010). Some synergism was observed in the U87MG-luc2 cell line (MGMT-expressing) as also previously reported (Voss *et al*, 2010). Nevertheless, U373 (MGMT-low level) and U251 (MGMT-negative) GBM cell lines (Chahal *et al*, 2012) demonstrated additive and antagonistic response to combined drug treatment. Interestingly, it has previously been reported that U251 and U373 GBM cell line express low Mcl-1 levels (Day *et al*, 2011), whereas U87 and U343 cell lines exhibit high Mcl-1 expression levels (Hetschko *et al*, 2008; Day *et al*, 2011; Murphy *et al*, 2014). We hypothesise that Mcl-1 may impact sensitivity to gossypol regimens. The efficacy of combined treatment may also be dependent on LDH expression in a given cell line as in single-agent gossypol treatment (Le *et al*, 2010; Seliger *et al*, 2013). Combined gossypol and TMZ treatment in endothelial cells again exhibited greater sensitivity when compared with tumour cell lines. This effect was confirmed in an *in vitro* endothelial cell–tube-formation assay (Figure 3). Greater drug synergism in HUVECs was also observed. It has previously been shown that tumour-associated endothelial cells express higher levels of the Bcl-2 gene than normal endothelial cells (Kaneko *et al*, 2007), resulting in enhanced angiogenesis and tumour growth (Nor *et al*, 2001). Moreover, it has further been shown that gossypol modulates VEGF signalling-mediated angiogenesis partially contributing to *in vivo* suppression of prostate tumour growth. A potent inhibitory effect of gossypol on VEGF-induced endothelial cell motility was also observed in human prostate cancer xenografts (Pang *et al*, 2011).

We also investigated whether gossypol and TMZ combination could suppress the invasive behaviour of GBM cells. 3-D spheroid invasion and 3-D matrigel trans-well invasion assays were employed in order to mimic the complexity and pathophysiology of *in vivo* tumour invasion. A significant anti-invasion response to combined treatment was observed in both assays (Figure 4 and Supplementary Figure S1). Potent anti-invasive properties of combined gossypol/TMZ treatment observed *in vitro* may be due to perturbation of MMP-2 activity via inhibition of Bcl-2 (gossypol) and TGF- β 2 (TMZ). This hypothesis is based on previously reported data, which indicates that (i) Bcl-2 proteins may promote tumour cell migration and invasion via induction of matrix metalloproteinase-2 (MMP-2) and cell surface urokinase-type plasminogen activator (uPA) (Wick *et al*, 1998; Choi *et al*, 2005; Trisciuglio *et al*, 2005), (ii) transforming growth factor-beta 2

(TGF- β 2) enables GBM cell infiltration via regulation of the expression of MMPs and α V β 3 integrin (Wick *et al*, 2002; Bruna *et al*, 2007) and that (iii) TMZ may inhibit (TGF- β 2)-induced invasiveness of GSCs (Zhang *et al*, 2011). The molecular mechanism by which Bcl-2 promotes MMP-2 and uPA induction has not yet been elucidated. However, as Bcl-2 and other anti-apoptotic Bcl-2 family proteins are increasingly recognised as physiological regulators of mitochondrial fusion/fission dynamics, mitochondrial bioenergetics and ER/mitochondrial Ca²⁺ homeostasis (Kilbride and Prehn, 2013), these may be complex. Clearly, these 'non-apoptotic' functions of Bcl-2 and their potential inhibition by gossypol, which binds to the BH3 binding groove of Bcl-2 family members, warrant further investigation. Indeed, BH3 peptides have been shown to induce mitochondrial fission independent of Bax/Bak-dependent apoptosis signalling (Shroff *et al*, 2009).

We also implemented a GBM xenograft model to test the combination of gossypol and TMZ *in vivo*. Significantly reduced tumour burden was observed in animals treated with combination gossypol/TMZ (after 2 weeks), when compared with single-agent gossypol therapy. However, no significant reduction in tumour volume was evident for combination gossypol therapy vs treatment with TMZ alone. Nevertheless, we observed a reduced number of animals presenting with visible tumour necrosis in the treatment groups, particularly in the gossypol/TMZ-combined cohort (Figure 5D). This observation may indicate that tumour cell proliferation (as evident via Ki67 staining) is decreased following combined treatment leading to slower tumour growth and reduced tumour core necrosis. As previously reported (Soling *et al*, 2004; Heikkilä *et al*, 2010; Goldman *et al*, 2011), we also observed extensive tumour necrosis in control tumours (Figure 5C) likely due to the rapid proliferation of U87MG-luc2 GBM cells when delivered SQ. Histopathological analysis showed that tumours from gossypol-treated animals have a similar histological architecture to control tumours. Furthermore, combination therapy does not manifest as a histologically distinct phenotype when tumours are compared with those from the single-agent TMZ treatment group. Moreover, tumours treated with either a single or combined regimen had decreased numbers of mitotic figures (Figure 5E). This indicates that tumour cell division is inhibited by gossypol and/or TMZ and is in line with other reports (Wolter *et al*, 2006; Filippi-Chiela *et al*, 2013; Shen *et al*, 2014). Examining more closely viable tumour histology in the non-necrotic regions, a significant decrease in proliferation was observed following combined gossypol/TMZ treatment as determined by Ki-67 staining, whereas a significant increase in the percentage of apoptotic cells was seen in the gossypol/TMZ combination treatment group as determined by TUNEL staining (Figure 5E, F and G). This suggests that the activity of gossypol and TMZ combined elicits cytotoxic and anti-proliferative effects *in vivo*. PECAM-1 staining of tumour tissue sections revealed a decrease in MVD (Figure 5E and H) underscoring the anti-angiogenic response of combined treatment observed *in vitro* (Figure 3).

In order to investigate combined gossypol/TMZ therapy in more clinically relevant patient-derived models and taking into account GBM heterogeneity, we examined treatment effects in three primary GBM cultures: patient-derived multicellular spheroid cultures (Jarzabek *et al*, 2013a) and neurospheres derived from two patients with differing MGMT clinical status (BT224-luc2—methylated MGMT and BT248-luc2—unmethylated MGMT). We observed greater resistance to TMZ treatment in patient-derived multicellular spheroids and neurosphere cultures when compared with adherent cell lines. Nevertheless, combined treatment enhanced primary GBM cell death when compared with TMZ alone. Extent of response varied for individual patients tested (Figure 6) likely due to differences in tumour molecular fingerprints. The genetic profiles of primary GBM biopsy and

in vivo multicellular spheroids showed typical GBM aberrations, such as: homozygous deletion of the PIK3R1 gene on chromosome 5; amplification of chromosome 7 including EGFR; homozygous deletion of CDKN2A/B and loss of one copy of chromosome 9; and homozygous deletion of chromosome 10 including the PTEN gene as described previously (Keunen *et al*, 2011) (Figure 6A, Supplementary Table S1). Among neurosphere lines (Figure 6B and C), we observed a greater decrease in cell viability in BT224-luc2 following gossypol alone and gossypol/TMZ combined treatment. This line, in contrast to BT248-luc2, showed methylated MGMT clinical status and no homozygous deletion of CDKN2A/B (Supplementary Table S1).

In summary, data presented herein indicate that implementing of a gossypol/TMZ combined regimen may be of relevance in the context of GBM. As presented, gossypol when combined with TMZ targets multiple 'hallmarks of cancer' (tumour proliferation, cell death and angiogenesis), which may provide benefit in patients presenting with advanced malignancies. Nevertheless, the extent of synergy observed is likely to be patient dependent. Mcl-1 and MGMT status may effect treatment outcome. Our data support further investigation of gossypol/TMZ combined approach in clinically relevant orthotopic models and ultimately in human trials.

ACKNOWLEDGEMENTS

We kindly acknowledge Professor Rolf Bjerkvig for providing GBM patient-derived spheroids. Funding is acknowledged from the Higher Education Authority Program in Research in Third Level Institution Cycle 4 (National Biophotonics Imaging Platform Ireland), FP7 AngioTox Industry Academic Pathways and Partnerships initiative (www.angiotox.com) and Science Foundation Ireland in the context of the Molecular Therapeutics for Cancer Ireland Strategic Research Cluster to ATB and WMG and Investigator Awards 08/IN.1/B1949 and 13/IA/1881 to JHMP.

CONFLICT OF INTEREST

The authors declare no conflict of interest.

REFERENCES

- Adams JM, Cory S (2007) Bcl-2-regulated apoptosis: mechanism and therapeutic potential. *Curr Opin Immunol* **19**: 488–496.
- Asai A, Miyagi Y, Sugiyama A, Gamanuma M, Hong SH, Takamoto S, Nomura K, Matsutani M, Takakura K, Kuchino Y (1994) Negative effects of wild-type p53 and s-Myc on cellular growth and tumorigenicity of glioma cells. Implication of the tumor suppressor genes for gene therapy. *J Neurooncol* **19**: 259–268.
- Azmi AS, Mohammad RM (2009) Non-peptidic small molecule inhibitors against Bcl-2 for cancer therapy. *J Cell Physiol* **218**: 13–21.
- Biroccio A, Candiloro A, Mottolese M, Sapora O, Albini A, Zupi G, del Bufalo D (2000) Bcl-2 overexpression and hypoxia synergistically act to modulate vascular endothelial growth factor expression and *in vivo* angiogenesis in a breast carcinoma line. *FASEB J* **14**: 652–660.
- Bjerkvig R, Tonnesen A, Laerum OD, Backlund EO (1990) Multicellular tumor spheroids from human gliomas maintained in organ culture. *J Neurosurg* **72**: 463–475.
- Bruna A, Darken RS, Rojo F, Ocana A, Penuelas S, Arias A, Paris R, Tortosa A, Mora J, Baselga J, Seoane J (2007) High TGF β -Smad activity confers poor prognosis in glioma patients and promotes cell proliferation depending on the methylation of the PDGF-B gene. *Cancer Cell* **11**: 147–160.
- Bushnow P, Reidenberg MM, Wasenko J, Winfield J, Lorenzo B, Lemke S, Himpler B, Corona R, Coyle T (1999) Gossypol treatment of recurrent adult malignant gliomas. *J Neurooncol* **43**: 79–86.

- Chahal M, Abdulkarim B, Xu Y, Guiot MC, Easaw JC, Stifani N, Sabri S (2012) O6-Methylguanine-DNA methyltransferase is a novel negative effector of invasion in glioblastoma multiforme. *Mol Cancer Ther* **11**: 2440–2450.
- Chipuk JE, Moldoveanu T, Llambi F, Parsons MJ, Green DR (2010) The BCL-2 family reunion. *Mol Cell* **37**: 299–310.
- Choi J, Choi K, Benveniste EN, Rho SB, Hong YS, Lee JH, Kim J, Park K (2005) Bcl-2 promotes invasion and lung metastasis by inducing matrix metalloproteinase-2. *Cancer Res* **65**: 5554–5560.
- Chou TC, Talalay P (1984) Quantitative analysis of dose-effect relationships: the combined effects of multiple drugs or enzyme inhibitors. *Adv Enzyme Regul* **22**: 27–55.
- Connors R, Schambach F, Read J, Cameron A, Sessions RB, Vivas L, Easton A, Croft SL, Brady RL (2005) Mapping the binding site for gossypol-like inhibitors of *Plasmodium falciparum* lactate dehydrogenase. *Mol Biochem Parasitol* **142**: 137–148.
- Coyle T, Levante S, Shetler M, Winfield J (1994) In vitro and in vivo cytotoxicity of gossypol against central nervous system tumor cell lines. *J Neurooncol* **19**: 25–35.
- Day BW, Stringer BW, Spanevello MD, Charmsaz S, Jamieson PR, Ensby KS, Carter JC, Cox JM, Ellis VJ, Brown CL, Walker DG, Inglis PL, Allan S, Reynolds BA, Lickliter JD, Boyd AW (2011) ELK4 neutralization sensitizes glioblastoma to apoptosis through downregulation of the anti-apoptotic protein Mcl-1. *Neuro-oncol* **13**: 1202–1212.
- del Duca D, Werbowetski T, del Maestro RF (2004) Spheroid preparation from hanging drops: characterization of a model of brain tumor invasion. *J Neurooncol* **67**: 295–303.
- Fernandez A, Udagawa T, Schwesinger C, Beecken W, Achilles-Gerte E, McDonnell T, D'amato R (2001) Angiogenic potential of prostate carcinoma cells overexpressing bcl-2. *J Natl Cancer Inst* **93**: 208–213.
- Filippi-Chiela EC, Thome MP, Bueno E Silva MM, Pelegrini AL, Ledur PF, Garicochea B, Zamin LL, Lenz G (2013) Resveratrol abrogates the temozolamide-induced G2 arrest leading to mitotic catastrophe and reinforces the temozolamide-induced senescence in glioma cells. *BMC Cancer* **13**: 147.
- Goldman SJ, Chen E, Taylor R, Zhang S, Petrosky W, Reiss M, Jin S (2011) Use of the ODD-luciferase transgene for the non-invasive imaging of spontaneous tumors in mice. *PLoS One* **6**: e18269.
- Gomez-Manzano C, Fueyo J, Kyritsis AP, McDonnell TJ, Steck PA, Levin VA, Yung WK (1997) Characterization of p53 and p21 functional interactions in glioma cells en route to apoptosis. *J Natl Cancer Inst* **89**: 1036–1044.
- Heikkilä JE, Vaha-Koskela MJ, Ruotsalainen JJ, Martikainen MW, Stanford MM, Mccart JA, Bell JC, Hinkkanen AE (2010) Intravenously administered alphavirus vector VA7 eradicates orthotopic human glioma xenografts in nude mice. *PLoS One* **5**: e8603.
- Hetschko H, Voss V, Senft C, Seifert V, Prehn JH, Kogel D (2008) BH3 mimetics reactivate autophagic cell death in anoxia-resistant malignant glioma cells. *Neoplasia* **10**: 873–885.
- Huang YW, Wang LS, Dowd MK, Wan PJ, Lin YC (2009) (-)-Gossypol reduces invasiveness in metastatic prostate cancer cells. *Anticancer Res* **29**: 2179–2188.
- Inda MM, Bonavia R, Mukasa A, Narita Y, Sah DW, Vandenberg S, Brennan C, Johns TG, Bachoo R, Hadwiger P, Tan P, Depinho RA, Cavenee W, Furnari F (2010) Tumor heterogeneity is an active process maintained by a mutant EGFR-induced cytokine circuit in glioblastoma. *Genes Dev* **24**: 1731–1745.
- Jarzabek MA, Huszthy PC, Skaftnesmo KO, McCormack E, Dicker P, Prehn JH, Bjerkvig R, Byrne AT (2013a) In vivo bioluminescence imaging validation of a human biopsy-derived orthotopic mouse model of glioblastoma multiforme. *Mol Imaging* **12**: 161–172.
- Jarzabek MA, Sweeney KJ, Evans RL, Jacobs AH, Stupp R, O'brien D, Berger MS, Prehn JH, Byrne AT (2013b) Molecular imaging in the development of a novel treatment paradigm for glioblastoma (GBM): an integrated multidisciplinary commentary. *Drug Discov Today* **18**: 1052–1066.
- Javed MH, Khan MA (1999) Effect of amino acids on inhibition of lactate dehydrogenase-X by gossypol. *Exp Mol Med* **31**: 25–29.
- Jiang J, Slivova V, Jedinak A, Sliva D (2011) Gossypol inhibits growth, invasiveness, and angiogenesis in human prostate cancer cells by modulating NF-kappaB/AP-1 dependent- and independent-signaling. *Clin Exp Metastasis* **29**: 165–178.
- Johannessen TC, Wang J, Skaftnesmo KO, Sakariassen PO, Enger PO, Petersen K, Oyan AM, Kalland KH, Bjerkvig R, Tysnes BB (2009) Highly infiltrative brain tumours show reduced chemosensitivity associated with a stem cell-like phenotype. *Neuropathol Appl Neurobiol* **35**: 380–393.
- Kaneko T, Zhang Z, Mantellini MG, Karl E, Zeitlin B, Verhaegen M, Soengas MS, Lingen M, Strieter RM, Nunez G, Nor JE (2007) Bcl-2 orchestrates a cross-talk between endothelial and tumor cells that promotes tumor growth. *Cancer Res* **67**: 9685–9693.
- Keunen O, Johansson M, Oudin A, Sanzey M, Rahim SA, Fack F, Thorsen F, Taxt T, Bartos M, Jirik R, Miletic H, Wang J, Stieber D, Stuhr L, Moen I, Rygh CB, Bjerkvig R, Niclou SP (2011) Anti-VEGF treatment reduces blood supply and increases tumor cell invasion in glioblastoma. *Proc Natl Acad Sci USA* **108**: 3749–3754.
- Kilbride SM, Prehn JH (2013) Central roles of apoptotic proteins in mitochondrial function. *Oncogene* **32**: 2703–2711.
- Koivunen P, Lee S, Duncan CG, Lopez G, Lu G, Ramkissoon S, Losman JA, Joensuu P, Bergmann U, Gross S, Travins J, Weiss S, Looper R, Ligon KL, Verhaak RG, Yan H, Kaelin Jr WG (2012) Transformation by the (R)-enantiomer of 2-hydroxyglutarate linked to EGLN activation. *Nature* **483**: 484–488.
- Krakstad C, Chekenya M (2010) Survival signalling and apoptosis resistance in glioblastomas: opportunities for targeted therapeutics. *Mol Cancer* **9**: 135.
- Kumar P, Ning Y, Polverini PJ (2008) Endothelial cells expressing Bcl-2 promotes tumor metastasis by enhancing tumor angiogenesis, blood vessel leakiness and tumor invasion. *Lab Invest* **88**: 740–749.
- Kwiatkowska A, Didier S, Fortin S, Chuang Y, White T, Berens ME, Rushing E, Eschbacher J, Tran NL, Chan A, Symons M (2012) The small GTPase RhoG mediates glioblastoma cell invasion. *Mol Cancer* **11**: 65.
- Le A, Cooper CR, Gouw AM, Dinavahi R, Maitra A, Deck LM, Royer RE, Vander Jagt DL, Semenza GL, Dang CV (2010) Inhibition of lactate dehydrogenase A induces oxidative stress and inhibits tumor progression. *Proc Natl Acad Sci USA* **107**: 2037–2042.
- Leonard EC, Friedrich JL, Basile DP (2008) VEGF-121 preserves renal microvessel structure and ameliorates secondary renal disease following acute kidney injury. *Am J Physiol Renal Physiol* **295**: F1648–F1657.
- Louis DN, Ohgaki H, Wiestler OD, Cavenee WK, Burger PC, Jouvet A, Scheithauer BW, Kleihues P (2007) The 2007 WHO classification of tumours of the central nervous system. *Acta Neuropathol* **114**: 97–109.
- Mehta S, Huillard E, Kesari S, Maire CL, Golebiowski D, Harrington EP, Alberta JA, Kane MF, Theisen M, Ligon KL, Rowitch DH, Stiles CD (2011) The central nervous system-restricted transcription factor Olig2 opposes p53 responses to genotoxic damage in neural progenitors and malignant glioma. *Cancer Cell* **19**: 359–371.
- Meng Y, Tang W, Dai Y, Wu X, Liu M, Ji Q, Ji M, Pienta K, Lawrence T, Xu L (2008) Natural BH3 mimetic (-)-gossypol chemosensitizes human prostate cancer via Bcl-xL inhibition accompanied by increase of Puma and Noxa. *Mol Cancer Ther* **7**: 2192–2202.
- Mohammad RM, Wang S, Aboukameel A, Chen B, Wu X, Chen J, Al-Katib A (2005) Preclinical studies of a nonpeptidic small-molecule inhibitor of Bcl-2 and Bcl-X(L) [(-)-gossypol] against diffuse large cell lymphoma. *Mol Cancer Ther* **4**: 13–21.
- Murphy AC, Weyhenmeyer B, Noonan J, Kilbride SM, Schimansky S, Loh KP, Kogel D, Letai AG, Prehn JH, Murphy BM (2014) Modulation of Mcl-1 sensitizes glioblastoma to TRAIL-induced apoptosis. *Apoptosis* **19**: 629–642.
- Nor JE, Christensen J, Liu J, Peters M, Mooney DJ, Strieter RM, Polverini PJ (2001) Up-Regulation of Bcl-2 in microvascular endothelial cells enhances intratumoral angiogenesis and accelerates tumor growth. *Cancer Res* **61**: 2183–2188.
- Onishi M, Ichikawa T, Kurozumi K, Date I (2011) Angiogenesis and invasion in glioma. *Brain Tumor Pathol* **28**: 13–24.
- Pang X, Wu Y, Lu B, Chen J, Wang J, Yi Z, Qu W, Liu M (2011) (-)-Gossypol suppresses the growth of human prostate cancer xenografts via modulating VEGF signaling-mediated angiogenesis. *Mol Cancer Ther* **10**: 795–805.
- Pedretti M, Verpelli C, Marland J, Bertani G, Sala C, Neri D, Bello L (2010) Combination of temozolomide with immunocytokine F16-IL2 for the treatment of glioblastoma. *Br J Cancer* **103**: 827–836.
- Qian SZ, Wang ZG (1984) Gossypol: a potential antifertility agent for males. *Annu Rev Pharmacol Toxicol* **24**: 329–360.
- Qiu J, Levin LR, Buck J, Reidenberg MM (2002) Different pathways of cell killing by gossypol enantiomers. *Exp Biol Med* **227**: 398–401.
- Ren Y, Zhou X, Mei M, Yuan XB, Han L, Wang GX, Jia ZF, Xu P, Pu PY, Kang CS (2010) MicroRNA-21 inhibitor sensitizes human glioblastoma

- cells U251 (PTEN-mutant) and LN229 (PTEN-wild type) to taxol. *BMC Cancer* **10**: 27.
- Rubin JB, Kung AL, Klein RS, Chan JA, Sun Y, Schmidt K, Kieran MW, Luster AD, Segal RA (2003) A small-molecule antagonist of CXCR4 inhibits intracranial growth of primary brain tumors. *Proc Natl Acad Sci USA* **100**: 13513–13518.
- Sauvageot CM, Weatherbee JL, Kesari S, Winters SE, Barnes J, Dellagatta J, Ramakrishna NR, Stiles CD, Kung AL, Kieran MW, Wen PY (2009) Efficacy of the HSP90 inhibitor 17-AAG in human glioma cell lines and tumorigenic glioma stem cells. *Neuro-oncol* **11**: 109–121.
- Seliger C, Leukel P, Moeckel S, Jachnik B, Lottaz C, Kreutz M, Brawanski A, Proescholdt M, Bogdahn U, Bosserhoff AK, Vollmann-Zwerenz A, Hau P (2013) Lactate-modulated induction of THBS-1 activates transforming growth factor (TGF)-beta2 and migration of glioma cells in vitro. *PLoS One* **8**: e78935.
- Shen W, Hu JA, Zheng JS (2014) Mechanism of temozolamide-induced antitumour effects on glioma cells. *J Int Med Res* **42**: 164–172.
- Shroff EH, Snyder CM, Budinger GR, Jain M, Chew TL, Khuon S, Perlman H, Chandel NS (2009) BH3 peptides induce mitochondrial fission and cell death independent of BAX/BAK. *PLoS One* **4**: e5646.
- Singh SK, Clarke ID, Terasaki M, Bonn VE, Hawkins C, Squire J, Dirks PB (2003) Identification of a cancer stem cell in human brain tumors. *Cancer Res* **63**: 5821–5828.
- Singh SK, Hawkins C, Clarke ID, Squire JA, Bayani J, Hide T, Henkelman RM, Cusimano MD, Dirks PB (2004) Identification of human brain tumour initiating cells. *Nature* **432**: 396–401.
- Soling A, Theiss C, Jungmichel S, Rainov NG (2004) A dual function fusion protein of Herpes simplex virus type 1 thymidine kinase and firefly luciferase for noninvasive in vivo imaging of gene therapy in malignant glioma. *Genet Vaccines Ther* **2**: 7.
- Stupp R, Hegi ME, MASON WP, Van Den Bent MJ, Taphoorn MJ, Janzer RC, Ludwin SK, Allgeier A, Fisher B, Belanger K, Hau P, Brandes AA, Gijtenbeek J, Marosi C, Vecht CJ, Mokhtari K, Wesseling P, Villa S, Eisenhauer E, Gorlia T, Weller M, Lacombe D, Cairncross JG, Mirimanoff RO (2009) Effects of radiotherapy with concomitant and adjuvant temozolamide versus radiotherapy alone on survival in glioblastoma in a randomised phase III study: 5-year analysis of the EORTC-NCIC trial. *Lancet Oncol* **10**: 459–466.
- Stupp R, Mason WP, Van den Bent MJ, Weller M, Fisher B, Taphoorn MJ, Belanger K, Brandes AA, Marosi C, Bogdahn U, Curschmann J, Janzer RC, Ludwin SK, Gorlia T, Allgeier A, Lacombe D, Cairncross JG, Eisenhauer E, Mirimanoff RO (2005) Radiotherapy plus concomitant and adjuvant temozolamide for glioblastoma. *N Engl J Med* **352**: 987–996.
- Trisciuglio D, Desideri M, Ciuffreda L, Mottolese M, Ribatti D, Vacca A, del Rosso M, Marcocci L, Zupi G, del Bufalo D (2005) Bcl-2 overexpression in melanoma cells increases tumor progression-associated properties and in vivo tumor growth. *J Cell Physiol* **205**: 414–421.
- Tuszynski GP, Cossu G (1984) Differential cytotoxic effect of gossypol on human melanoma, colon carcinoma, and other tissue culture cell lines. *Cancer Res* **44**: 768–771.
- Voss V, Senft C, Lang V, Ronellenfitsch MW, Steinbach JP, Seifert V, Kogel D (2010) The pan-Bcl-2 inhibitor (-)-gossypol triggers autophagic cell death in malignant glioma. *Mol Cancer Res* **8**: 1002–1016.
- Wang J, Miletic H, Sakariassen PO, Huszthy PC, Jacobsen H, Brekka N, Li X, Zhao P, Mork S, Chekenya M, Bjerkvig R, Enger PO (2009) A reproducible brain tumour model established from human glioblastoma biopsies. *BMC Cancer* **9**: 465.
- Wick W, Wagner S, Kerkau S, Dichgans J, Tonn JC, Weller M (1998) BCL-2 promotes migration and invasiveness of human glioma cells. *FEBS Lett* **440**: 419–424.
- Wick W, Wick A, Schulz JB, Dichgans J, Rodemann HP, Weller M (2002) Prevention of irradiation-induced glioma cell invasion by temozolamide involves caspase 3 activity and cleavage of focal adhesion kinase. *Cancer Res* **62**: 1915–1919.
- Wolter KG, Wang SJ, Henson BS, Wang S, Griffith KA, Kumar B, Chen J, Carey TE, Bradford CR, D'silva NJ (2006) (-)-gossypol inhibits growth and promotes apoptosis of human head and neck squamous cell carcinoma in vivo. *Neoplasia* **8**: 163–172.
- Xu L, Yang D, Wang S, Tang W, Liu M, Davis M, Chen J, Rae JM, Lawrence T, Lippman ME (2005) (-)-Gossypol enhances response to radiation therapy and results in tumor regression of human prostate cancer. *Mol Cancer Ther* **4**: 197–205.
- Zhang D, Jing Z, Qiu B, Wu A, Wang Y (2011) Temozolamide decreases invasion of glioma stem cells by down-regulating TGF-beta2. *Oncol Rep* **26**: 901–908.
- Ziegler DS, Keating J, Kesari S, Fast EM, Zavel L, Ramakrishna N, Barnes J, Kieran MW, Veldhuijzen van Zanten SE, Kung AL (2011) A small-molecule IAP inhibitor overcomes resistance to cytotoxic therapies in malignant gliomas in vitro and in vivo. *Neuro-oncol* **13**: 820–829.

This work is published under the standard license to publish agreement. After 12 months the work will become freely available and the license terms will switch to a Creative Commons Attribution-NonCommercial-Share Alike 3.0 Unported License.

Supplementary Information accompanies this paper on British Journal of Cancer website (<http://www.nature.com/bjc>)